42 600; CD (c 4.81 × 10^{-4}, cyclohexane) $\Delta\epsilon_{232}$ −20.24, $\Delta\epsilon_{217}$ −12.92, $\Delta\epsilon_{200}$ −9.03. Anal. Calcd for $C_{20}H_{22}O_4$: C, 73.62; H, 6.75. Found: C, 73.65; H, 6.88.

(*Z*)-(1*R*)-(4(a)-(Benzoyloxy)-2-adamantylidene)propene (34). (*Z*)-(1*R*)-(4(a)-Hydroxy-2-adamantylidene)propene[11] (**33**) (20 mg, $[\alpha]^{25}_{Hg}$ +25.23 ± 0.31°, 84% ee) was benzoylated as earlier to give 29 mg of (*Z*)-(1*R*)-(4(a)-(benzoyloxy)-2-adamantylidene)propene (**34**) as a colorless liquid: $[\alpha]^{25}_{Hg}$ −168.69 ± 0.08° (c 0.57, $CHCl_3$); IR (CCl_4) 3070 (w), 3050 (w), 3030 (w), 2910, 2850, 1800 (w), 1717, 1655, 1600, 1580 (w), 1450, 1340, 1320, 1275, 1180, 1120, 1100–900 cm^{-1}; ^1H NMR δ 1.60–2.10 (m, 8 H), 2.20 (br d, 1 H), 2.22 (br s, 1 H), 2.44 (br s, 1 H), 3.31 (br s, 1 H), 4.88 (dd, *J* = 1.83, 10.37 Hz, 1 H), 5.09 (dd, *J* = 1.83, 16.78 Hz, 1 H), 5.26 (br s, 1 H), 5.98 (d, *J* = 10.98 Hz, 1 H), 6.52 (sextet, *J* = 10.38, 10.99, 16.48 Hz, 1 H), 7.33–7.59 (m, 3 H), 7.96 (dd, *J* = 1.83, 8.54 Hz, 2 H); ^{13}C NMR, see ref 11; UV (c 4.28 × 10^{-5}, 4.28 × 10^{-4}, cyclohexane) λ_{320} ε 150, λ_{304} ε 280, λ_{280} ε 1000, λ_{273} ε 1138, λ_{267} ε 1054, λ_{247} ε 17 600, λ_{238} ε 30 300, λ_{230} ε 35 700, λ_{195} ε 43 900; CD (c 4.28 × 10^{-4}, 4.28 × 10^{-3}, cyclohexane) $\Delta\epsilon_{318}$ −0.075, $\Delta\epsilon_{304}$ −0.11, $\Delta\epsilon_{279}$ −0.82, $\Delta\epsilon_{272}$ −1.03, $\Delta\epsilon_{265}$ −0.89, $\Delta\epsilon_{237}$ −43.40, $\Delta\epsilon_{219}$ +15.75, $\Delta\epsilon_{195}$ +38.50. Anal. Calcd for $C_{20}H_{22}O_2$: C, 81.63; H, 7.48. Found: C, 81.70; H, 7.50.

(*E*)-(1*R*)-(4(a)-(Benzoyloxy)-2-adamantylidene)propene (30). Following an earlier procedure,[11] 10 mg of (*E*)-(1*R*)-(4(a)-hydroxy-2-adamantylidene)propene (**29**) ($[\alpha]^{25}_{Hg}$ +16.76 ± 3.30°, 84% ee) was benzoylated to yield 14 mg of pure (*E*)-(1*R*)-(4(a)-(benzoyloxy)-2-adamantylidene)propene (**30**): $[\alpha]^{26}_{Hg}$ −78.03 ± 0.40° (c 0.27, $CHCl_3$); IR ($CHCl_3$) 2920, 2860, 1715, 1655, 1605 (w), 1590 (w), 1470–1460, 1350, 1325, 1285, 1185–910 cm^{-1}; ^1H NMR δ 1.70–2.30 (m, 10 H), 2.64 (br s, 1 H), 3.07 (br s, 1 H), 4.97 (m, *J* = 0.64, 2.07, 10.15 Hz, 1 H), 5.10 (m, *J* = 0.61, 2.07, 17.23 Hz, 1 H), 5.26 (br s, 1 H), 5.79 (d, *J* = 10.92 Hz, 1 H), 6.65 (sextet, *J* = 10.20, 10.63, 16.84 Hz, 1 H), 7.30–7.60 (m, 3 H), 8.00 (dd, *J* = 2.04, 7.51 Hz, 2 H); UV (c 3.97 × 10^{-5}, 3.97 × 10^{-4}, cyclohexane) λ_{279} ε 1200, λ_{272} ε 1300, λ_{265} ε 1186, λ_{248} ε 14 100, λ_{238} ε 25 400, λ_{228} ε 31 200, λ_{196} ε 48 800; CD (c 3.97 × 10^{-4}, 3.97 × 10^{-3}, cyclohexane) $\Delta\epsilon_{278}$ −0.62, $\Delta\epsilon_{271}$ −0.74, $\Delta\epsilon_{288}$ −21.11, $\Delta\epsilon_{220}$ +8.97. Anal. Calcd for $C_{20}H_{22}O_2$: C, 81.63; H, 7.48. Found: C, 82.00; H, 7.80.

(*Z*)-(1*R*)-(4(e)-(Benzoyloxy)-2-adamantylidene)propene (42). Benzoylation of (*Z*)-(1*R*)-(4(e)-hydroxy-2-adamantylidene)propene[11] (**41**) (10 mg, $[\alpha]^{26}_{Hg}$ +31.65 ± 1.07°, 84% ee) as described earlier gave after purification 13 mg of (*Z*)-(1*R*)-(4(e)-(benzoyloxy)-2-adamantylidene)-propene (**42**): $[\alpha]^{26}_{Hg}$ +74.94 ± 0.23° (c 0.44, $CHCl_3$); IR ($CHCl_3$) 2920, 2860, 1715, 1650, 1605, 1590, 1470, 1460, 1355, 1325, 1285, 1130, 1100–910 cm^{-1}; ^1H NMR δ 1.60–2.40 (m, 10 H), 2.42 (br s, 1 H), 3.28 (br s, 1 H), 5.00 (dd, *J* = 2.05, 10.10 Hz, 1 H), 5.08 (br s, 1 H), 5.16 (dd, *J* = 1.99, 16.65 Hz, 1 H), 5.90 (d, *J* = 10.98 Hz, 1 H), 6.62 (sextet, *J* = 10.45, 10.67, 16.86 Hz, 1 H), 7.40–7.65 (m, 3 H), 8.10 (dd, *J* = 1.51, 8.86 Hz, 2 H); UV (c 5.61 × 10^{-5}, 5.61 × 10^{-4}, cyclohexane) λ_{279} ε 780, λ_{271} ε 969, λ_{247} ε 19 700, λ_{237} ε 34 600, λ_{232} ε 35 800, λ_{196} ε 43 500; CD (c 5.61 × 10^{-4}, 5.61 × 10^{-3}, cyclohexane) $\Delta\epsilon_{279}$ +0.18, $\Delta\epsilon_{271}$ +0.38, $\Delta\epsilon_{238}$ +21.91, $\Delta\epsilon_{221}$ −15.10. Anal. Calcd for $C_{20}H_{22}O_2$: C, 81.63; H, 7.48. Found: C, 81.76; H, 7.19.

(*E*)-(1*R*)-(4(e)-(Benzoyloxy)-2-adamantylidene)propene (38). By use of a previous procedure,[11] (*E*)-(1*R*)-(4(e)-hydroxy-2-adamantylidene)-propene (**37**) (8 mg, $[\alpha]^{26}_{Hg}$ +29.44 ± 1.67°, 84% ee) was benzoylated to yield after purification 10 mg of (*E*)-(1*R*)-(4(e)-(benzoyloxy)-2-adamantylidene)propene (**38**): $[\alpha]^{26}_{Hg}$ +21.94 ± 0.46° (c 0.29, $CHCl_3$); IR ($CHCl_3$) 2920, 2860, 1718, 1650, 1590, 1470, 1460, 1350, 1325, 1286, 1128, 1020–910 cm^{-1}; ^1H NMR δ 1.60–2.40 (m, 10 H), 2.67 (br s, 1 H), 3.03 (br s, 1 H), 5.02 (dd, *J* = 1.97, 10.20 Hz, 1 H), 5.12 (br s, 1 H), 5.17 (dd, *J* = 1.51, 16.10 Hz, 1 H), 5.90 (d, *J* = 11 Hz, 1 H), 6.61 (sextet, *J* = 10.45, 10.62, 16.82 Hz, 1 H), 7.40–7.60 (m, 3 H), 8.10 (m, 2 H); UV (c 2.58 × 10^{-5}, 2.58 × 10^{-4}, cyclohexane) λ_{279} ε 790, λ_{271} ε 980, λ_{247} ε 16 500, λ_{238} ε 28 500, λ_{232} ε 29 400, λ_{195} ε 37 600; CD (c 2.58 × 10^{-4}, 2.58 × 10^{-3}, cyclohexane) $\Delta\epsilon_{279}$ +0.14, $\Delta\epsilon_{271}$ +0.28, $\Delta\epsilon_{238}$ +15.78, $\Delta\epsilon_{220}$ −9.98. Anal. Calcd for $C_{20}H_{22}O_2$: C, 81.63; H, 7.48. Found: C, 81.66; H, 7.71.

Acknowledgment. We thank Prof. J. Brewster, Purdue University, who, serving as a referee, made substantial contributions to the clarity of this article. We are indebted to him. This work was supported by a grant from the National Science Foundation, to whom we are grateful.

Characterization of the Copper Sites in *Pseudomonas perfectomarina*[1] Nitrous Oxide Reductase by Resonance Raman Spectroscopy

David M. Dooley,*[2a] Richard S. Moog,[2a,b] and Walter G. Zumft[2c]

Contribution from the Department of Chemistry, Amherst College, Amherst, Massachusetts 01002, and Lehrstuhl für Mikrobiologie, Universität Karlsruhe, D-7500 Karlsruhe 1, Federal Republic of Germany. *Received November 10, 1986*

Abstract: Several unusual copper chromophores are observed in various forms of *Pseudomonas perfectomarina* nitrous oxide reductase. Resonance Raman spectroscopy at 290 and 77 K has been used to characterize some of the copper sites in the resting and reduced forms of this enzyme. Eleven to twelve fundamentals are observed at 77 K with 514.5-nm excitation, consistent with resonance enhancement for both metal–ligand stretches and internal ligand deformations. Comparisons to resonance Raman spectra of blue (type 1) copper proteins and Cu(II)-substituted liver alcohol dehydrogenase indicate that the 540-nm chromophore of resting N_2O reductase likely is associated with a $Cu^{II}S_2(cys)_2N(his)$ site. No evidence was found for contributions from Cu^{II}–tyrosine units or from an organic coenzyme to the visible absorption spectra. The low-activity resting form contains a copper site that displays a resonance Raman spectrum similar to those observed for blue copper sites; the high-activity form apparently does not contain such a site. Variations in the enzymatic activity of resting N_2O reductase may correlate with the number of 540-nm chromophores present. When either resting form is reduced by ascorbate or dithionite, new blue forms ($\lambda_{max} \simeq 650$ nm) are produced. Reduced N_2O reductase displays a resonance Raman spectrum that is, at least, very similar to that of the low-activity resting form obtained with 633-nm excitation. The circular dichroism spectrum of reduced N_2O reductase resembles the CD spectra of several blue copper proteins, with regard to band energies and intensities. It is likely that reduced N_2O reductase contains an oxidized copper site that is inaccessible to external, anionic reductants.

Denitrification is the reduction of nitrate to dinitrogen, as schematically illustrated below:[3]

$$2NO_3^- \rightarrow 2NO_2^- \rightarrow 2NO \rightarrow N_2O \rightarrow N_2 \qquad (1)$$

Although important to balancing the global nitrogen cycle, denitrification is a biologically (and economically) expensive process, since it returns fixed nitrogen (nitrate is readily reduced to ammonia by many organisms) to the atmosphere. Recently, certain

(1) Transfer of *Pseudomonas perfectomarina* to *Pseudomonas stutzeri* has recently been proposed. See: Döhler, K.; Huss, V. A. R.; Zumft, W. G. *Int. J. Syst. Bacteriol.* **1987**, *37*, 1–3.

(2) (a) Amherst College. (b) Present address: Department of Chemistry, Franklin and Marshall College. (c) Universität Karlsruhe.

(3) Payne, W. J. *Denitrification*; Wiley: New York, 1981.

(4) Delwiche, C. C., Ed. *Denitrification, Nitrification, and Atmospheric Nitrous Oxide*; Wiley: New York, 1981.

(5) Knowles, R. *Microbiol. Rev.* **1982**, *46*, 43–70.

0002-7863/87/1509-6730$01.50/0

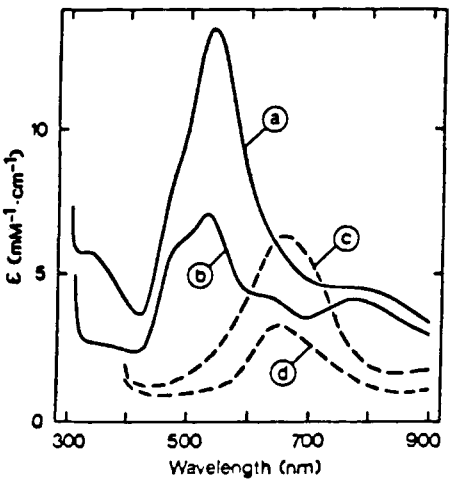

Figure 1. Electronic spectra of the different forms of N_2O reductase from *P. perfectomarina*. (a) Enzyme as isolated under anaerobic conditions (purple form); (b) enzyme as isolated under aerobic conditions (pink form); (c) spectrum as in spectrum a after addition of excess dithionite; (d) spectrum as in spectrum b after addition of excess dithionite. All spectra were recorded in 25 mM Tris/HCl, pH 7.5. Reprinted with permission from ref 12.

nitrite reductases and nitrous oxide reductases have been shown to be copper-containing metalloenzymes.[6-13] Heme-containing nitrite reductases are also known,[3-5,14] but all the nitrous oxide reductases purified to date are multicopper enzymes. *Pseudomonas perfectomarina* nitrous oxide reductase is the best characterized.[11,12] N_2O can serve as the terminal electron acceptor in this organism, with N_2O reductase catalyzing the overall two-electron reduction (eq 2).[11,12] Denitrifying organisms couple

$$N_2O + 2e^- + 2H^+ \rightarrow N_2 + H_2O \qquad (2)$$

nitrate, nitrite, and nitrous oxide reduction to ATP synthesis. The enzyme contains 6–8 coppers per protein molecule (M_r = 120000), which is composed of two identical subunits.[12] Anaerobic, potentiometric titrations established the midpoint potential as +260 mV (SHE, 25 °C, pH 7.5). Resting *P. perfectomarina* N_2O reductase displays an unusual EPR spectrum with a seven-line copper hyperfine in the $g_\parallel$ region; EPR spin-Hamiltonian parameters are $g_\parallel = 2.18$ ($A_\parallel = 38.3$G), $g_\perp = 2.03$ ($A_\perp = 28$G).[12] However, only 65 ± 5% of the copper is EPR detectable. The absorption spectra (Figure 1) are also unusual and, together with the EPR results, suggest that novel copper centers may be present. N_2O reductase can be isolated in high-activity and low-activity forms that display distinct electronic absorption spectra.[11,12] Moreover, dithionite reduction yields new forms with absorption spectra that are very similar to the spectra of classic "blue" copper proteins. Clearly, the magnitudes of the extinction coefficients indicate that the electronic transitions in Figure 1 are electric dipole allowed, and hence probably charge transfer in nature, although the presence of an organic cofactor has not been definitively excluded. Inspecting Figure 1 (spectrum a is the high-activity form; spectrum b is the low-activity form) suggests that the catalytic activity is correlated with the novel 540-nm chromophore. However, the high-activity form may be further activated about tenfold, by increasing the pH from 7.5 to ~10, without altering the absorption spectrum.[12]

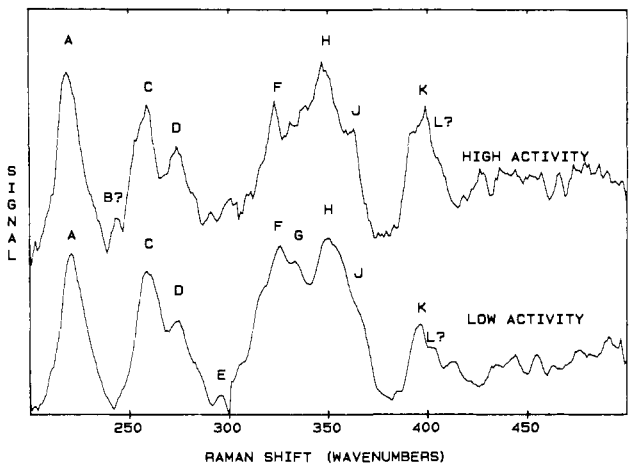

Figure 2. Room temperature (~290 K) resonance Raman spectra of the high- and low-activity forms of resting N_2O reductase in Tris buffer, pH 7.5. Laser wavelength = 514.5 nm.

It seems likely that the copper sites in N_2O reductase are structured differently than the well-known type 1, type 2, and type 3 sites in copper proteins. There is no indication in the EPR spectrum that type 2 copper is present in N_2O reductase. The EPR and electronic absorption spectra of N_2O reductase are quite different than blue (type 1) copper spectra. Copper–copper interactions are suggested by the $A_\parallel$ pattern and the integrated EPR intensity; hence the possibility that type 3 copper is present must be considered. We have begun extensive spectroscopic studies of the N_2O reductase in order to characterize the structural and electronic properties of its copper sites. Resonance Raman spectroscopy is a particularly informative probe of copper sites in proteins.[15] Blue copper proteins have been extensively investigated by this physical method; the basic features of blue copper resonance Raman spectra are reasonably well-understood.[16-23] These results form a very useful base for interpreting the spectra from new systems. In this paper we describe resonance Raman spectroscopic studies of *P. perfectomarina* N_2O reductase, under ambient and cryogenic conditions, which indicate that a new type of Cu(II)–sulfur chromophore is present.

Experimental Section

N_2O reductase was isolated from *P. perfectomarina* as previously described[12] and displayed properties (electrophoretic behavior, activity) consistent with high purity. Samples for Raman spectroscopy were concentrated initially by ultrafiltration (Amicon membrane) and then

(6) Masuko, M.; Iwasaki, H.; Sakurai, T.; Suzuki, S.; Nakahara, A. *J. Biochem.* **1984**, *96*, 447–454.
(7) (a) Iwasaki, H.; Matsubara, T. *J. Biochem.* **1972**, *71*, 645–652. (b) Iwasaki, H.; Noji, S.; Shidara, S. *J. Biochem.* **1975**, *78*, 355–361.
(8) Kakutani, T.; Watanabe, H.; Arima, K.; Beppu, T. *J. Biochem.* **1981**, *89*, 453–461.
(9) Michalski, W. P.; Nicholas, D. J. D. *Biochim. Biophys. Acta* **1985**, *828*, 130–137.
(10) DiSpirito, A. A.; Taaffe, L. R.; Lipscomb, J. D.; Hooper, A. B. *Biochim. Biophys. Acta* **1985**, *827*, 320–326.
(11) (a) Zumft, W. G.; Matsubara, T. *FEBS Lett.* **1982**, *148*, 107–112. (b) Matsubara, T.; Zumft, W. G. *Arch. Microbiol.* **1982**, *132*, 322–328. (c) Zumft, W. G.; Coyle, C. L.; Frunzke, K. *FEBS Lett.* **1985**, *183*, 240–244.
(12) Coyle, C. L.; Zumft, W. G.; Kroneck, P. M.; Körner, H.; Jakob, W. *Eur. J. Biochem.* **1985**, *153*, 459–467.
(13) Matsubara, T.; Sano, M. *Chem. Lett.* **1985**, 1053–1056.
(14) Shapleigh, J. P.; Payne, W. J. *FEMS Microbiol. Lett.* **1985**, *26*, 275–279.
(15) Loehr, T. M.; Sanders-Loehr, J. In *Copper Proteins and Copper Enzymes*; Lontie, R., Ed.; CRC: Boca Raton, FL, 1984; Vol. I, pp 115–155.
(16) (a) Siiman, O.; Young, N. M.; Carey, P. R. *J. Am. Chem. Soc.* **1976**, *96*, 5583–5588. (b) Siiman, O.; Young, N. M.; Carey, P. R. *J. Am. Chem. Soc.* **1976**, *98*, 744–749.
(17) Miskowski, V. M.; Tang, S.-P.; Spiro, T. G.; Shapiro, E.; Moss, T. H. *Biochemistry* **1975**, *14*, 1244–1249.
(18) Nestor, L.; Larrabee, J. A.; Woolery, G.; Reinhammar, B.; Spiro, T. G. *Biochemistry* **1984**, *23*, 1084–1093.
(19) Nestor, L.; Reinhammar, B.; Spiro, T. G. *Biochim. Biophys. Acta* **1986**, *869*, 286–292.
(20) (a) Woodruff, W. H.; Norton, K. A.; Swanson, B. I.; Fry, H. A. *J. Am. Chem. Soc.* **1983**, *105*, 657–662. (b) Woodruff, W. H.; Norton, K. A.; Swanson, B. I.; Fry, H. A. *Proc. Natl. Acad. Sci. U.S.A.* **1984**, *81*, 1263–1267.
(21) Blair, D. F.; Campbell, G. W.; Schoonover, J. R.; Chan, S. I.; Gray, H. B.; Malström, B. G.; Pecht, I.; Swanson, B. I.; Woodruff, W. H.; Cho, W. K.; English, A. M.; Fry, H. A.; Lum, V.; Norton, K. A. *J. Am. Chem. Soc.* **1985**, *107*, 5755–5766.
(22) Thamann, T. J.; Frank, P.; Willis, L. J.; Loehr, T. M. *Proc. Natl. Acad. Sci. U.S.A.* **1982**, *79*, 6396–6400.
(23) Blair, D. F.; Campbell, G. W.; Lum, V.; Martin, C. T.; Gray, H. B.; Malmström, B. G.; Chan, S. I. *J. Inorg. Biochem.* **1983**, *19*, 65–73.

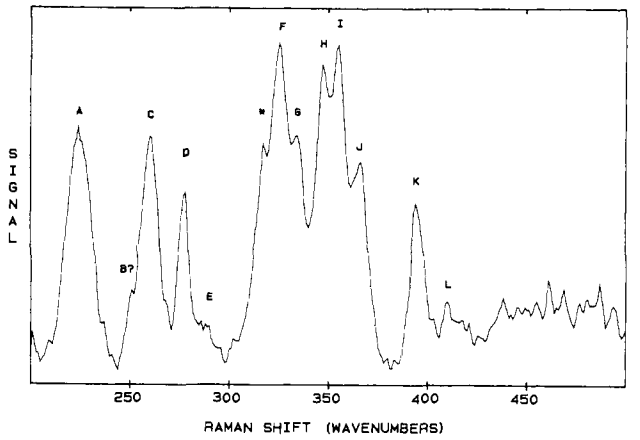

Figure 3. 77 K resonance Raman spectrum of the low-activity form of resting N_2O reductase in Tris buffer, pH 7.5. Laser wavelength = 514.5 nm. The feature marked with an asterisk (*) is probably a weak ice band.

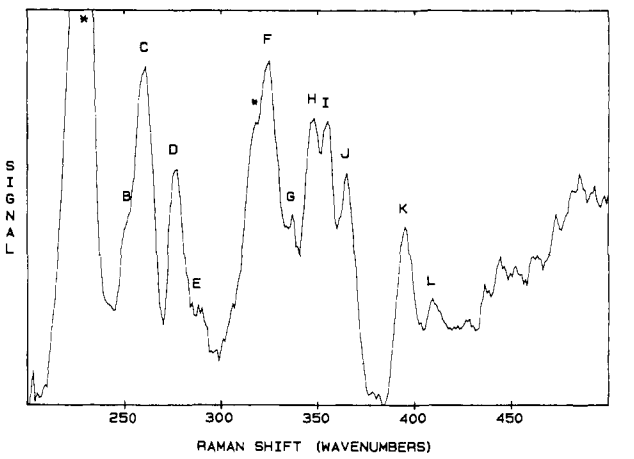

Figure 4. 77 K resonance Raman spectrum of the high-activity form of resting N_2O reductase, in Tris buffer, pH 9.8. Laser wavelength = 514.5 nm. The feature marked with an asterisk (*) is probably a weak ice band. Note that the peak at ~220 cm^{-1} is overlapped by an ice band in this spectrum, leading to anomalously high intensity.

further concentrated via slow evaporation at 4 °C in a desiccator. Final copper concentrations were generally ≥1 mM. Samples were exchanged into D_2O buffers by 4–5 cycles of concentration in an Amicon stirred-cell, followed by dilution with ~10 volumes of D_2O buffer. Raman spectra were obtained with a Spex Ramalog system (UV–vis illuminator, 0.85-m monochromator, cooled Hamamatsu R928 photomultiplier) interfaced to a Spex Datamate and an IBM PC. A beam-splitter and photodiode were employed to generate a reference signal used to correct the data for temporal fluctuations in the laser intensity. Coherent INNOVA 18 Ar^+ and CR-599 dye lasers provided the exciting lines. Samples were placed in glass capillaries for data collection at ambient temperature. Spectra were collected at 77 K with use of a custom dewar (Lab Glass) fitted with optical flats. Sealed capillaries containing the samples were directly immersed in liquid N_2. A slow flow of He gas into the N_2 bath prevented vigorous boiling. In all cases the scattered light was collected at 90° from the incident direction and focussed through a polarization scrambler onto the monochromator slits. The spectral bandwidth was 4 cm^{-1} and data were collected in 1-cm^{-1} increments. Typically, counts were averaged for 1 s per point at ambient temperature and 2.0 s per point at 77 K. Several scans were collected, examined for consistency, and averaged. The data were smoothed by using a standard routine and, when necessary, linear backgrounds were subtracted. Only bands that were reproducible between scans *and* independent experiments are marked in the figures. We have found that the Raman spectra themselves provide the most sensitive indication of photochemically or thermally induced degradation of the N_2O reductase. Laser powers were 10–50 mW for ambient temperature experiments and ~100 mW (at the dewar window) for the 77 K experiments.

Results

Figure 2 shows the room temperature resonance Raman spectra of the high- and low-activity forms of N_2O reductase, obtained with 514.5-nm excitation. The spectra are clearly very similar, but some minor differences in the relative intensities and resolution are evident; in part these differences may be attributed to the lower signal-to-noise ratio in the spectrum of the high-activity form, particularly in the 300–370-cm^{-1} region. Resonance Raman spectra at 77 K are shown in Figures 3 and 4. These spectra are much better resolved than those obtained at ambient temperature, as is also the case for blue copper proteins and Cu(II)-substituted liver alcohol dehydrogenase (LADH).[24] At least 11–12 fundamentals are observed at 77 K, the majority of which are also observed at room temperature. The frequencies of all bands observed with 514.5-nm excitation are collected in Table I. Only peak D shifted significantly (−2 cm^{-1}) when spectra were obtained from D_2O solutions. No significant differences are apparent in the high-activity form at pH 9.8 and 7.5. Comparison of the room temperature and 77 K spectra suggests that no major temperature-dependent conformational changes occur that affect the

Table I. Resting N_2O Reductase Frequencies (cm^{-1}) Observed with 514.5-nm Excitation[a]

band	low-activity form (290 K)	high-activity form (290 K)	low-activity form (77 K)	high-activity form[b] (77 K)
A	221	219	224	*c*
B		245	249	252
C	259	259	260	261
D	275	274	278	276
E	296		289	288
F	326	323	325	325
G	333		334	337
H	350	347	347	348
I			355	355
J	363	363	366	365
K	396	399	394	395
L	405	409	410	409

[a] All values accurate to ±1 cm^{-1}; obtained at pH 7.5 except where noted. See Figures 2–4. [b] pH 9.8. [c] Obscured by the ice band at 230 cm^{-1}.

540-nm chromophore. Moreover, the variation in activity does not appear to be associated with structural variations in this chromophore. Thus the copper site(s) involved are *structurally* identical in the low- and high-activity forms, which suggests that catalytic activity may correlate with the *number* of 540-nm chromophores present.

All the vibrations evident in Figures 2–4 are enhanced by resonance with the 540-nm chromophore. Enhancement profiles indicate that none of the modes gain intensity via resonance with the 480-nm chromophore, ruling out the possibility that Figures 2–4 are composites containing contributions from different sites associated with the 480- and 540-nm absorption bands. There are many more peaks than can be plausibly assigned to copper–ligand stretching vibrations. Thus, internal ligand deformations must be resonantly enhanced, as is also the case in blue copper proteins.[18-22] A careful search in the 1000–1600-cm^{-1} region with 457.9, 476.5, and 514.5-nm excitation revealed no bands as intense as the non-enhanced phenylalanine ring breathing mode at 1001 cm^{-1}. Since excitation of a tyrosine → Cu(II) ligand-to-metal charge-transfer (LMCT) transition generally produces strong enhancements of ring modes,[25] Cu^{II}–tyrosine groups are unlikely to contribute to the absorption spectra (Figure 1). Further, the absence of bands in the 1000–1600-cm^{-1} region is inconsistent with the assignment of any low-energy electronic transition to an organic coenzyme. Since Cu^{II}–imidazole chromophores are not expected to display intense LMCT transitions below 20 000 cm^{-1}, even in near-tetrahedral geometries (see ref 26), the unusual N_2O

(24) (a) Maret, W.; Zeppezauer, M.; Sanders-Loehr, J.; Loehr, T. M. *Biochemistry* **1983**, *22*, 3202–3206. (b) Maret, W.; Shiemke, A. K.; Wheeler, W. D.; Loehr, T. M.; Sanders-Loehr, J. *J. Am. Chem. Soc.* **1986**, *108*, 6351–6359.

(25) Pyrz, J. W.; Karlin, K. D.; Sorrell, T. N.; Vogel, G. C.; Que, L., Jr. *Inorg. Chem.* **1984**, *23*, 4581–4584.

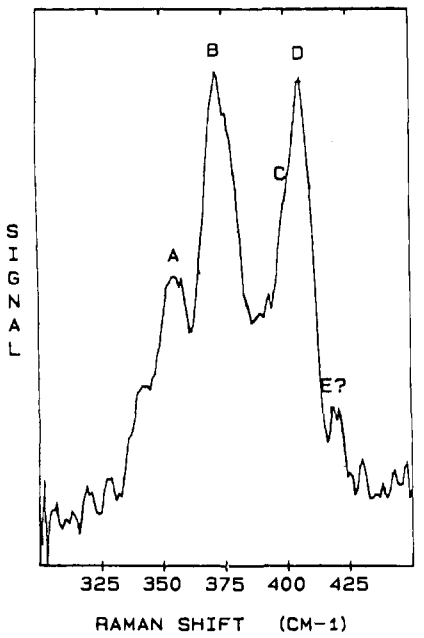

Figure 5. Room temperature (~290 K) resonance Raman spectrum of the low-activity form of resting N_2O reductase in Tris buffer, pH 7.5. Laser wavelength = 633 nm.

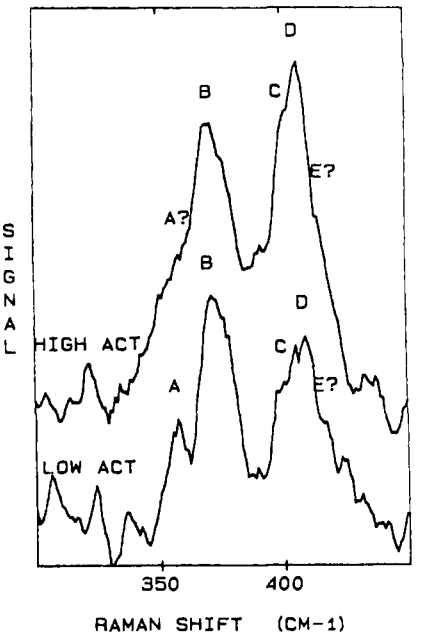

Figure 6. Room temperature (~290 K) resonance Raman spectra of the dithionite reduced forms of N_2O reductase in Tris buffer, pH 7.5. Spectra of the ascorbate reduced forms were identical. Laser wavelength = 633 nm.

reductase electronic absorption spectra must be associated with Cu^{II}–sulfur bonding, probably with cysteine(s). However, the N_2O reductase spectra differ significantly from the resonance Raman spectra of proteins containing a blue copper center, with the possible exception of Cu^{II}–LADH. Most obviously, bands are evident at ~220 cm^{-1} and near 260 cm^{-1} in the N_2O reductase spectra, which are comparable in intensity to those at higher energy, whereas most blue copper proteins display only weak resonance Raman signals in the 200–300-cm^{-1} region.[16-23] Second, two moderately intense bands are observed between 300 and 330 cm^{-1} in both resting forms of the N_2O reductase; blue copper resonance Raman spectra have, at most, only weak features in this region.[16-23] However, Cu^{II}–LADH does display relatively intense peaks at 198 cm^{-1} (at 162 and 202 cm^{-1} for the NADH complex) and in the 300–330-cm^{-1} region.[24] Finally, the spectra in Figure 2–4 contain several peaks in the 330–420-cm^{-1} region. Although the most strongly enhanced normal modes of blue copper sites appear in this region, the frequencies are generally higher.

Figure 5 shows the resonance Raman spectrum of the low-activity form of N_2O reductase obtained with 633-nm excitation. This spectrum is distinctly different than that observed with 514.5-nm excitation (Figure 3), both with regard to the positions and relative intensities of the peaks: the most intense modes in Figure 5 are not present in Figure 3 and no modes in the 200–300-cm^{-1} region are observed. Hence the resonance Raman spectra and the corresponding absorption bands at 540 and 630 nm must be associated with different copper sites. Remarkably, the spectrum in Figure 5 shows considerable similarity to blue copper resonance Raman spectra, although the N_2O reductase frequencies are again somewhat lower. No resonantly enhanced modes are observed when the high-activity form is excited at 633 nm.

Reducing the resting forms of N_2O reductase with dithionite or ascorbate produces a blue form (Figure 1). This process is not strictly reversible as only the low-activity resting form is obtained upon reoxidation.[12] Although both blue species have λ_{max} = 650 nm, the extinction coefficients at this wavelength are 3400 and 6100 M^{-1} cm^{-1} when prepared from the low-activity and high-activity forms, respectively. Resonance Raman spectra for both blue forms are shown in Figure 6. Only ambient temperature spectra were measured, and the relatively poor signal to noise in these data precludes a detailed analysis. Clearly, the two blue species have very similar resonance Raman spectra and therefore probably have the same structure. On the basis of the absorption spectra, the number of copper sites absorbing at 650 nm may be different in the two blue forms; the absorptivities are consistent with 1–2 such sites, given the range observed for established blue copper proteins. Comparing Figures 5 and 6 indicates that the copper sites in the blue species and the 630-nm chromophore in the low-activity resting form are at least very similar, if not

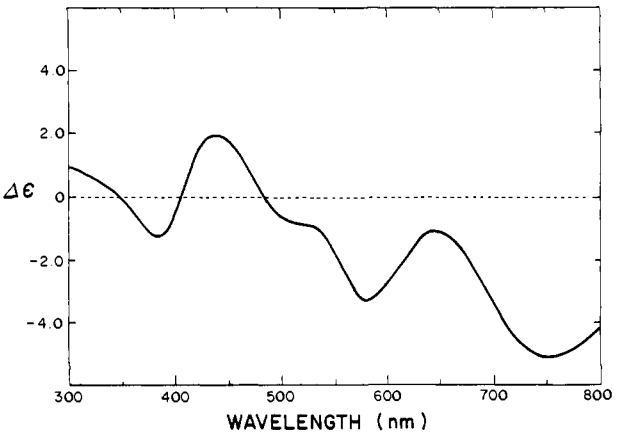

Figure 7. Room temperature (~295 K) CD spectrum of dithionite-reduced N_2O reductase in Tris buffer, pH 7.5. This sample was prepared from the low-activity resting form.

Table II. Frequencies (cm^{-1}) Observed with 633-nm Excitation of the Low-Activity Resting Form and the Reduced Forms of N_2O Reductase[a]

band	low-activity form (290 K)	reduced low-activity form (290 K)	reduced high-activity form (290 K)
A	355	358	357
B	372	371	371
C	398	401	400
D	406	406	409
E	419	415	417

[a] All values accurate to ±2 cm^{-1}, see Figures 5–7.

(26) Schugar, H. J. In *Copper Coordination Chemistry: Biochemical and Inorganic Perspectives*; Karlin, K. D., Zubieta, J., Eds.; Adenine: Guilderland, NY; 1983, pp 43–74 and references cited therein.

(27) (a) Heller, E. J. *Acc. Chem. Res.* **1981**, *14*, 368–375. (b) Heller, E. J.; Sundberg, R. L.; Tannor, D. *J. Phys. Chem.* **1982**, *86*, 1822–1833.

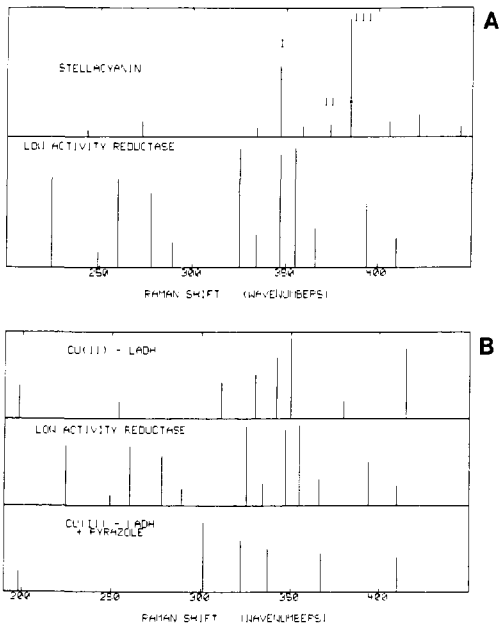

Figure 8. Line representations of the 77 K resonance Raman spectra of stellacyanin (A), Cu^{II}–LADH (B), and resting N_2O reductase (A and B). The stellacyanin and LADH data are taken from ref 18 and 35, respectively.

identical. Raman frequencies for these sites are collected in Table II. The CD spectrum of reduced N_2O reductase is shown in Figure 7 for comparison to the CD spectra of blue copper proteins (vide infra).

Discussion

Stellacyanin and Cu^{II}–LADH display Cu–S Raman frequencies that correspond more closely to N_2O reductase frequencies than those of other blue copper proteins. A comparison between the resonance Raman spectra of stellacyanin, Cu^{II}–LADH, and N_2O reductase is found in Figure 8. The generally lower frequencies observed for stellacyanin, compared to other blue copper proteins, are thought to be related to the longer Cu–S bond in stellacyanin, namely, 2.19 Å versus 2.10–2.13 Å.[18,21] It is clear that modes in the N_2O reductase spectrum can be correlated with stellacyanin modes known to contain substantial Cu–S stretching character (I–III, Figure 8). In both spectra the bands in the 330–410-cm^{-1} region are strongly enhanced, indicating that the modes are coupled to the resonant electronic transitions, known to be a $S(\sigma) \rightarrow Cu^{II}$–LMCT transition in stellacyanin.[28] This points to a Cu^{II}–S bond in the 540-nm chromophore that is an analogue of the Cu^{II}–S bond in stellacyanin, that is, with a bond length of ~2.2 Å (or longer).

All blue copper resonance Raman spectra have a peak at ca. 270 cm^{-1} that has been assigned as a Cu–N(his) stretch.[17,18,21] Peak D (Figures 2–4) can be assigned to this mode in N_2O reductase. The deuterium isotope shift (−2 cm^{-1}) is consistent with such an assignment.[18,21] Additionally, the intensity of peak D is noticeably temperature dependent, being relatively more intense at 77 K than at ~300 K. Similar behavior is well documented for the Cu–N(his) stretch in azurin.[20,21]

Assignments for peaks A–C are certainly of interest but more problematic. Previous work has shown that the principal source for resonance Raman intensity in the vibrations of the blue copper chromophore is very likely the fractional contribution from the Cu–S(cys) stretch.[18,21,24] Since the 540-nm band of N_2O reductase is also almost certainly a $S(\sigma) \rightarrow Cu^{II}$–LMCT transition, comparisons to the Raman spectra of Cu^{II}–LADH and certain $Cu^{II}N_2S_2$ model complexes (vide infra) suggest some plausible assignments. Weak features present in the 100–250-cm^{-1} region in the resonance Raman spectra of blue copper proteins have not yet been assigned. Cu^{II}–LADH and some of its complexes display one or two peaks between 160 and 200 cm^{-1} that are significantly more intense than the low-frequency modes (100–250 cm^{-1}) of other blue copper proteins, using the high-frequency Cu–S modes as standards.[24] It is apparent that N_2O reductase displays three relatively intense peaks at 220, 260, and 278 cm^{-1} and that the Cu^{II}–LADH resonance Raman spectrum has two peaks in this region. As discussed above, one of these peaks is assigned as a Cu–N(his) stretch in both spectra. Furthermore, the resonance Raman spectra of the two proteins in the 300–425-cm^{-1} region are also similar. Some spectral properties of the Cu^{II}–LADH–pyrazole complex resemble those of resting N_2O reductase. On the basis of its absorption spectrum (λ_{max} = 505 nm) and EPR parameters ($g_\parallel$ = 2.20, $g_\perp$ = 2.05, $A_\parallel \cong$ 110 G), the pyrazole complex has a more tetragonal geometry than Cu^{II}–LADH.[24,32] Solvent nuclear magnetic relaxation dispersion measurements are consistent with a five-coordinate structure for the Cu(II) ion in Cu^{II}–LADH–pyrazole.[33] Except for $A_\parallel$, for which no satisfactory interpretation is yet available for N_2O reductase, the pyrazole complex of Cu^{II}–LADH may be a potentially useful model for the novel copper sites in N_2O reductase. Their resonance Raman spectra are different, however (Figure 8), perhaps suggesting that the N_2O reductase site is not five-coordinate. On balance, such comparisons suggest that the copper sites associated with the 540-nm chromophore in N_2O reductase share some structural similarities with distorted tetrahedral Cu^{II}–S_2N site in Cu^{II}–LADH. The higher energy of the LMCT transition in N_2O reductase (540 nm vs. ~600 nm) implies that the N_2O reductase site is less tetrahedrally distorted (more tetragonal). Loehr and co-workers have not assigned any peaks in the Cu^{II}–LADH spectra to vibrations of the individual cysteinate ligands. Peaks in the 300–425-cm^{-1} region may reflect vibrations of both Cu–S(cys) units in Cu^{II}–LADH and N_2O reductase, whereas the peaks at low frequencies could arise from modes involving S–Cu–S deformations.[31] Further work is necessary to clarify these points, but the Raman data indicate that there are both overall structural similarities and some differences between the Cu^{II}–LADH sites and the 540-nm-absorbing copper sites in N_2O reductase. Additional support for the presence of two cysteine ligands to Cu(II) in the 540-nm chromophore of N_2O reductase comes from the spectroscopic properties of a distorted tetrahedral $Cu^{II}S_2N_2$ complex.[34] This complex displays an intense $S(\sigma) \rightarrow Cu^{II}$–LMCT transition at 535 nm (e = 3000 L^{-1} M^{-1}). The room temperature resonance Raman spectrum obtained with 514.5-nm excitation[35] is similar in several respects to the N_2O reductase spectrum shown in Figure 2.

A second type of copper site ($\lambda_{max} \sim$ 630 nm) is present in the low activity form and might be produced by the transformations that lead to the decrease in activity, as the absorptivity at 630 nm is higher relative to that at 540 nm in the low-activity as compared to the high-activity form (Figure 1). No resonantly enhanced bands were observed with 630-nm excitation of the high-activity resting form. One possibility, suggested by work on Cu^{II}–LADH,[24,32] is that changes in geometry or the number of non-cysteine ligands may convert a 540-nm chromophore to a 630-nm chromophore in N_2O reductase. It is remarkable that

(28) Solomon, E. I.; Hare, J. W.; Dooley, D. M.; Dawson, J. H.; Stephens, P. J.; Gray, H. B. *J. Am. Chem. Soc.* **1980**, *102*, 168–173.
(29) Penfield, K. W.; Gewirth, A. A.; Solomon, E. I. *J. Am. Chem. Soc.* **1981**, *103*, 4382–4388.
(30) Penfield, K. W.; Gewirth, A. A., Solomon, E. I. *J. Am. Chem. Soc.* **1985**, *107*, 4519–4529.
(31) Woodruff, W. H.; Dyer, R. G.; Schoonover, J. R. In *Biological Applications of Raman Spectroscopy*; Spiro, T. G., Ed.; Wiley: New York, 1987; Vol. IV, in press.
(32) Maret, W.; Dietrich, H.; Ruf, H.-H.; Zeppezauer, M. *J. Inorg. Biochem.* **1980**, *12*, 241–252.
(33) Andersson, I.; Maret, W.; Zeppezauer, M.; Brown, R. D., III; Koening, S. H. *Biochemistry* **1981**, *20*, 3424–3432.
(34) Anderson, O. P.; Becher, J.; Fryendahl, H.; Taylor, L. F.; Toftlund, H. *J. Chem. Soc., Chem. Commun.* **1986**, 699–701.
(35) Jenson, W. P.; Becher, J.; Toftlund, H. In *Spectroscopy of Biological Molecules*; Alix, A. J. P., Bernard, L., Manfait, M., Eds.; Wiley: New York, 1985; pp 205–207.

the formation of a site that is apparently similar to a classic blue copper site (a site extremely well-suited for facile electron-transfer reactivity) is apparently associated with a decrease in the catalytic activity of N_2O reductase.

When either ascorbate or dithionite is used to reduce resting N_2O reductase, the resulting "blue" form displays an unusual EPR spectrum that is distinctly different from typical blue copper EPR signals.[36] This EPR spectrum and the blue absorbance persist even in solutions containing excess reductant.[12] Despite the implications of these observations, the vibrational frequencies and relative intensities in the resonance Raman spectrum of the blue form (Figure 6) are essentially identical with those of the "blue" copper chromophore in the resting form (Figure 5) and rather similar to the pattern in the resonance Raman spectra of other blue copper proteins. Furthermore, the CD spectrum (Figure 7) resembles the CD spectra of many blue copper proteins with regard to both the intensities and energies of the bands, although some differences in the signs are evident.[28] We suggest that at least one *oxidized* copper ion may be present in the *reduced* N_2O reductase prepared from either the low- or high-activity resting form. Type 1 copper ions invariably display positive (vs. SHE) reduction potentials, indicating that if the "blue" sites in N_2O reductase are similar, they must be inaccessible to negatively charged exogenous reductants. Because neither reduced form can apparently be reoxidized to the high-activity resting form, irreversible protein conformational changes may accompany reduction. These conformational changes may also render the "blue" sites inaccessible.

(36) Coyle, C. L.; Zumft, W. G.; Jakob, W.; Kroneck, P. M. H.; Zumft, W. G. *Rev. Port. Quim.* **1985**, *27*, 168–170.

Conclusions

The resonance Raman data indicate that the unusual spectroscopic properties of the *P. perfectomarina* N_2O reductase are associated with Cu–S chromophores. In particular, a $[Cu^{II}S_2(cys)_2N(his)]$ site is suggested to be responsible for the intense 540-nm absorption band of the resting forms; this absorption correlates with catalytic activity, implying that the novel copper site is essential for turnover. No organic coenzyme or Cu^{II}–tyrosine units contribute to the visible absorption spectrum. A copper that is similar to a classical blue copper ion is present in the low-activity form of the resting enzyme, but probably not in the high-activity form. This blue site might be an altered 540-nm chromophore. The incremental activation of the high-activity form by base is not associated with structural perturbations of the 540-nm chromophore, suggesting that the pH-induced changes that give rise to the increased activity are localized on another copper site or the protein moiety. Reduced N_2O reductase also contains a chromophore that resembles an oxidized blue copper ion, which is apparently inaccessible to external reductants.

Acknowledgment. We thank Tom Loehr, Joann Sanders-Loehr, Tom Spiro, Cathy Coyle, and Peter Kroneck for several helpful discussions and for communicating results in advance of publication. We also thank a reviewer and Associate Editor Sunney Chan for their constructive comments. Michele McGuirl and Sigrid Mümmler provided excellent technical assistance. This research was supported by the National Institutes of Health (Grant GM 27659 to D.M.D.) and the Deutsche Forschungsgemeinschaft (W.G.Z.). The acquisition of the laser Raman facility was made possible by a grant from the National Institutes of Health (1 S10 RRO 1569).

A Building Block for the Sequence-Specific Introduction of Cis–Syn Thymine Dimers into Oligonucleotides. Solid-Phase Synthesis of TpT[*c*,*s*]pTpT

John-Stephen Taylor,* Ian R. Brockie, and Christine L. O'Day

Contribution from the Department of Chemistry, Washington University, St. Louis, Missouri 63130. *Received September 29, 1986*

Abstract: We report the synthesis of a synthetic intermediate for the sequence specific incorporation of the cis–syn thymine dimer into oligonucleotides via phosphoramidite-based solid-phase DNA synthesis technology. The required phosphoramidite **1a** was obtained in four steps from the known, pT-$O_{3'}$-(*tert*-butyldimethylsilyl)thymidylyl-(3′→5′)-thymidine, *R*,*S*-*O*-methyl phosphate, compounds **6a**,**b**. Compounds **6a**,**b** were photolyzed with Pyrex-filtered light in the presence of the triplet sensitizer, acetophenone. The resulting four products, **12a**, **12b**, **8a**, and **8b**, were separated by a combination of flash chromatography and preparative reverse phase gradient HPLC. The structures of the four products were determined by complete deprotection and correlation with authentic cis–syn and trans–syn cyclobutane dimers of TpT, **9** and **13**, obtained from the photosensitized irradiation of thymidylyl-(3′→5′)-thymidine **7**. Compound **8a**, one of the two protected cis–syn isomers epimeric at phosphorus, was converted to the Tp-O_5-DMT derivative **10a**, followed by removal of the *tert*-butyldimethylsilyl group to give **11a**. Compound **11a** was converted to the target pT-$O_{3'}$-methyl morpholinylphosphonite **1a** which was purified by flash chromatography. The cis–syn thymine dimer containing phosphoramidite was coupled to thymidine derivatized controlled pore glass support and further extended by an additional thymidine. The methyl phosphate protecting groups were removed, and the resulting thymine dimer containing tetranucleotide **14** was obtained after cleavage from the support. Tetrathymidylate **15** was prepared in a similar fashion for comparison purposes. Photolysis of **14** at 254 nm gave **15** as the major photoreversion product, thus establishing the integrity of the cis–syn thymine dimer unit. Both oligonucleotides were characterized by ^1H and ^{31}P NMR spectroscopy, C-18 and anion exchange HPLC chromatography, high resolution gel electrophoresis, and by a chemical degradation sequence. It was also established that the cis–syn cyclobutane dimer of TpT was stable to the conditions required to remove the standard amino protecting groups of A, C, and G. This makes the building block **1a** applicable to the synthesis of cis–syn thymine dimer containing oligonucleotides of heterogeneous sequence.

Exposure of DNA to ultraviolet light leads to the formation of a variety of photoproducts, otherwise known as photolesions.[1] Victims of the inherited disorder *xeroderma pigmentosum* are extremely sensitive to sunlight and have an approximately thou-

0002-7863/87/1509-6735$01.50/0